

Analysis of decimation techniques to improve computational efficiency of a frequency-domain evaluation approach for real-time hybrid simulation

Tong Guo¹, Weijie Xu² and Cheng Chen^{*3}

¹Key Laboratory of Concrete and Prestressed Concrete Structures of the Ministry of Education, Southeast University, Nanjing, P.R. China

²School of Civil Engineering, Southeast University, Nanjing, P.R. China

³School of Engineering, San Francisco State University, San Francisco, CA, USA

(Received April 10, 2014, Revised August 15, 2014, Accepted August 20, 2014)

Abstract. Accurate actuator tracking is critical to achieve reliable real-time hybrid simulation results for earthquake engineering research. The frequency-domain evaluation approach provides an innovative way for more quantitative post-simulation evaluation of actuator tracking errors compared with existing time domain based techniques. Utilizing the Fast Fourier Transform the approach analyzes the actuator error in terms of amplitude and phase errors. Existing application of the approach requires using the complete length of the experimental data. To improve the computational efficiency, two techniques including data decimation and frequency decimation are analyzed to reduce the amount of data involved in the frequency-domain evaluation. The presented study aims to enhance the computational efficiency of the approach in order to utilize it for future on-line actuator tracking evaluation. Both computational simulation and laboratory experimental results are analyzed and recommendations on the two decimation factors are provided based on the findings from this study.

Keywords: real-time hybrid simulation; frequency-domain; computational efficiency; data decimation; frequency decimation

1. Introduction

Real-time hybrid simulation provides a novel and effective way to observe the behavior of critical elements at large- or full-scale when subjected to dynamic loading. In real-time hybrid simulation, the structure is split into experimental substructure(s) and analytical substructure(s), which are physically tested in the laboratory and numerically simulated in computer program respectively. The structural responses under external excitation are calculated by solving the dynamic equations of motion using an integration algorithm. The calculated displacement responses from the integration algorithm are converted to command displacements using delay compensation methods and then imposed onto the experimental substructure(s) using servo-hydraulic actuators. The restoring forces of the experimental substructures are sent back to

*Corresponding author, Assistant Professor, E-mail: chcsfsu@sfsu.edu

the integrate algorithm to calculate the next step displacement response. This process is repeated until the end of the ground motion. Under recent continuous developments, the real-time hybrid simulation technique has become a viable alternative to the more well-established shaking table testing and the pseudo-dynamic testing methods (Nakashima *et al.* 1992, Bonnet *et al.* 2007, Chen *et al.* 2010).

Unlike conventional experimental techniques such as quasi-static cyclic tests and quasi-static hybrid simulations, the command displacements in a real-time hybrid simulation are required to be imposed onto the experimental substructure(s) in a real-time manner. However, due to inherent servo-hydraulic dynamics, the actuator has an inevitable time delay in response to the displacement command, which is detrimental for both stability and accuracy of real-time hybrid simulations. Previous researches showed that the time delay would lead to inaccurate test results and even destabilize the entire simulation if not compensated properly (Horiuchi *et al.* 1999, Darby *et al.* 1999, Chen and Ricles 2007, Mercan 2007). Various compensation methods have been proposed to minimize the effect of actuator delay. Horiuchi *et al.* (1999) proposed compensation schemes for actuator delay which are based on polynomial extrapolation and linear acceleration assumption, respectively. Carrion and Spencer (2006) proposed a model based compensation method. Chen and Ricles (2007) proposed an inverse compensation derived through a discrete transfer function approach. These compensation methods assume constant time delay in real-time hybrid simulation and require accurate estimate of actuator delay. Darby *et al.* (2002) proposed a method to estimate the time delay by calculating the error between the measured and the desired actuator responses. Ahmadzadeh *et al.* (2008) proposed to estimate time delay by using the average of last three measured and calculated displacements instead of the measured and calculated displacements themselves. These two time delay estimation methods are both based on time domain and need to find a proper gain before the simulation. Moreover, when actuator delay varies throughout the simulation, constant delay compensation methods would lead to under- or over-compensation. To solve this problem, compensation methods based on adaptive control theory are explored to adjust the compensation parameter in real-time hybrid simulation, such as the adaptive inverse compensation (AIC) method (Chen and Ricles 2010, Chen *et al.* 2012) and the feedforward-feedback tracking control (Phillips *et al.* 2011).

Experimental studies show that the effects of servo-hydraulic dynamics can be reduced but cannot be completely eliminated even when the most sophisticated compensation method is used (Chen *et al.* 2010, Chen and Ricles 2010, Chen *et al.* 2012). This poses a significant challenge not only to minimize the effect of actuator delay during the test but also to post-simulation assessment of experimental results. Since the true structural response is often not available after the experiment, it is necessary to conduct post-simulation actuator tracking assessment to properly interpret the real-time hybrid simulation results for the seismic performances of the structures under investigation. Most existing evaluation methods are formulated in the time domain to evaluate the errors between calculated displacements and measured displacements. Some of these include the maximum tracking error (*MTE*), root-mean-square (*RMS*) of the tracking error, the tracking indicator (*TI*) (Mercan 2007, Chen and Ricles 2010, Chen *et al.* 2010) and the energy error (*EE*) (Mosqueda *et al.* 2007a, b). These methods evaluated the actuator tracking throughout a real-time hybrid simulation by single parameter. Hessabi and Mercan (2012) developed a dual parameter evaluation method, i.e., the phase and amplitude error indices (*PAEI*), to identify the experimental errors by phase error and amplitude error through uncoupled closed-form equations. These time-domain based variables are very useful when applied to compare different delay compensation methods under same experimental scenario (Chen *et al.* 2010). Smaller values of

MTE, *RMS*, *TI* or *EE* often imply better actuator tracking. For the real-time hybrid simulations with the same ground motion input but scaled to different hazard levels, the same actuator dynamics could induce different values of *MTE*, *RMS*, *TI*, *PAEI* or *EE* due to the different command displacements for the actuators. Smaller values of *MTE*, *RMS*, *TI*, *PAEI* or *EE* thus do not necessarily represent better actuator tracking. The time-history dependence of *TI* and *EE* could also pose challenges for direct application for reliability assessment of real-time hybrid simulation results (Chen and Sharma 2012). An inaccurate estimate of delay estimate could result in large value of *TI* and *EE* but does not necessarily deviate the simulation response from actuator response (Chen and Ricles 2010).

To overcome the limitation of existing evaluation methods in time domain, Guo *et al.* (2013) proposed a frequency-domain based approach to interpret the actuator tracking in terms of amplitude error and phase error. A window transform function (Harris 1978) was used to minimize the effect of the spectrum leakage and the concept of the equivalent frequency was introduced to calculate the delay in the tests. This frequency-domain based approach was verified first by numerical simulation and laboratory tests of predefined displacements (Guo *et al.* 2013) and then by real-time hybrid simulation results (Chen *et al.* 2013a). Compared with time-domain based evaluation methods, the frequency-domain based evaluation approach provides more quantitative assessment of the effect of actuator delay throughout a real-time hybrid simulation. Its current form however is suitable only for post-simulation assessment. The fact that this approach requires the entire simulation data results in low computational efficiency and prevents its application for potential on-line monitoring of the effect of servo-hydraulic dynamics. To this end, this paper explored two numerical techniques to enhance its efficiency so that only partial experimental data are necessary for the frequency domain based approach to quickly and accurately identify the error in actuator tracking. Both computational simulation and experimental results from real-time hybrid simulation are used to evaluate the effectiveness of the two techniques.

2. Formulation of frequency-domain evaluation approach

The frequency-domain based approach developed by Guo *et al.* is first briefly described. Consider signals $I(t)$ and $O(t)$ as the calculated and measured displacements of the servo-hydraulic actuator in a real-time hybrid simulation, respectively. Transform these two signals from time domain to frequency domain using the Fast Fourier transform (*FFT*) transforms (Bracewell 2000), which can be expressed as

$$y_i(f) = \mathcal{F}[I(t)] \quad (1a)$$

$$y_o(f) = \mathcal{F}[O(t)] \quad (1b)$$

where f denotes the frequency; t is the time variable; \mathcal{F} represents the Fast Fourier transform; $y_i(f)$ and $y_o(f)$ represent the *FFT* of the input and output signals, respectively.

Assuming that amplitude error and time delay between output $O(t)$ and input $I(t)$ leads to

$$O(t) = K \cdot I(t - \tau) \quad (2)$$

where K and τ represent the amplitude error and time delay, respectively.

Applying *FFT* to Eq. (2) leads to

$$y_o(f) = K \cdot y_i(f) \cdot e^{-j \cdot 2\pi \cdot f \cdot \tau} \quad (3)$$

where j is the imaginary unit and is defined as $\sqrt{-1}$. Define $y_n(f) = y_o(f)/y_i(f)$, which then can be derived as

$$y_n(f) = K \cdot e^{-j \cdot 2\pi \cdot f \cdot \tau} \quad (4)$$

Using the Euler formula leads to

$$y_n(f) = K \cdot [\cos(-2\pi f \tau) + i \sin(-2\pi f \tau)] \quad (5)$$

The magnitude A_0 and the phase ϕ_0 of $y_n(f)$ can be obtained as

$$A_0 = \|y_n(f)\| = K \quad (6a)$$

$$\phi_0 = -\arctan(\sin(2\pi f \tau) / \cos(2\pi f \tau)) = -2\pi f \tau \quad (6b)$$

where $\|\cdot\|$ represents the modulus. From Eqs. (6(a)) and (6(b)), the amplitude and phase between calculated displacements and measured displacements can be calculated through the frequency response analysis and the accuracy of actuator tracking in a real-time hybrid simulation can thus be evaluated. The error between A_0 and 1 is the amplitude error of actuator tracking, and the error between ϕ_0 and 0 is the phase error. The smaller amplitude error and phase error, the more accurate of the actuator tracking and the more reliable of the real-time hybrid simulation results. Moreover, Eq. (6(b)) indicates that the time delay can be calculated by dividing the phase ϕ_0 by the frequency of the signal. For sinusoidal inputs and outputs with single dominant frequency, the value of f in Eq. (6(b)) can be easily identified as the frequency of the sinusoidal input. For signals with more than one dominant frequency, the concept of equivalent frequency f^{eq} is introduced for the calculation of time delay, which is defined as

$$f^{eq} = \frac{\sum_{i=1}^p (\|\mathcal{F}[I(t)]_i\|^l \cdot f_i)}{\sum_{i=1}^p \|\mathcal{F}[I(t)]_i\|^l} \quad (7)$$

where l is the number of the displacement signal in time domain and it depends on the data length of the displacements measured or calculated in the tests; and p is the number of frequencies to be considered and is equal to the half of smallest power of two that is greater than or equal to the number of data,

$$p = 2^{\text{nextpow2}(L)-1} \quad (8)$$

where L is the data length; the `nextpow2` function returns the smallest power of two that is greater than or equal to the absolute value of L (MATLAB 2009). The maximum value of f_i is the half of sampling frequency and can be calculated as $f_i = \Delta f L$, where the frequency interval Δf can be calculated as

$$\Delta f = \frac{f_s}{2p} \tag{9}$$

where f_s is the sampling rate for the real-time hybrid simulation. Thus when random signals are used, the difference between the input and output signals can also be evaluated using the amplitude A_0 in Eq. (6(a)) and ϕ_0 in Eq. (6(b)). Substituting Eq. (7) into Eq. (6(b)) leads to an equivalent delay, which can be calculated as

$$d = -\phi_0 / (2\pi \cdot f^{eq}) \tag{10}$$

The equivalent delay d in Eq. (10) represents the time delay between the input and output signals evaluated at the equivalent frequency. The generalized amplitude A and phase ϕ can be calculated as

$$A = \|FEI\| \tag{11a}$$

$$\phi = \arctan[\text{Im}(FEI) / \text{Re}(FEI)] \tag{11b}$$

where $\text{Im}(\cdot)$ and $\text{Re}(\cdot)$ represent the imaginary and real part of FEI , respectively; and FEI represents the weighted sum of $\mathcal{F}[I(t)]_j / \mathcal{F}[O(t)]_j$ ($j=1,2,\dots,p$) defined as

$$FEI = \sum_{j=1}^p \left\{ \frac{\mathcal{F}[O(t)]_j}{\mathcal{F}[I(t)]_j} \cdot \frac{\|\mathcal{F}[I(t)]_j\|^l}{\sum_{i=1}^p \|\mathcal{F}[I(t)]_i\|^l} \right\} \tag{12}$$

For real-time hybrid simulation, perfect actuator tracking implies that the measured actuator response is exactly the same as the command displacement. In this ideal circumstance, no time delay and amplitude error exist between the input and output, i.e., $d=0$ and $A=1$. It is worth noting that in Eqs. (7) and (12), the amplitude of FFT for each frequency under consideration is weighted by the same integer power l . Guo *et al.* indicated that a value of 2 for the parameter l provides good results.

It can also be observed from above that the frequency-domain evaluation approach requires that all the time-domain measured data be translated into frequency domain. The calculation of f^{eq} in Eq. (7) and FEI in Eq. (12) need to weigh all p frequencies with an interval of Δf . The resulted requirement of computational effort does not affect the post-simulation however brings challenges for the application of the approach towards real-time on-line tracking assessment. It is therefore necessary to improve the computational efficiency of the frequency based approach.

3. Data decimation factor P

For the frequency-domain approach, the computational efficiency is dependent on the amount of data acquired from real-time hybrid simulation. The state-of-the-art servo-hydraulic equipment could reach a sampling frequency as high as 2048 Hz. How to efficiently extract useful information from experimental data presents a challenge for the frequency-domain based approach. Resample the displacements from tests by decimation provides a possible way to reduce the amount of data so as to improve the computational efficiency. Using the MATLAB function

“decimate” (MATLAB 2009), the test data (calculated displacements, command displacements and measured displacements) can be resampled in time domain through an integer parameter of P , so as to reduce the maximum frequency without changing the frequency interval. Greater value of P results in less test data and higher computational efficiency.

3.1 Computational simulation

Both linear elastic and nonlinear structures are considered to verify the effectiveness of data decimation in improving the computational efficiency in a real-time hybrid simulation (Chen *et al.* 2014).

3.1.1 Linear elastic structure

For the purpose of analysis, a linear elastic single-degree-of-freedom (SDOF) structure is selected where the restoring force measurement from the actuator is calculated by multiplying the measured displacement by the linear elastic stiffness. For the real-time hybrid simulation, the restoring force associated with stiffness k is isolated as experimental substructure while the rest of the SDOF structure is modeled as analytical substructure. To eliminate possible effect of integration algorithms (Chen and Ricles 2007), a continuous transfer function in the Laplace domain is used. The fundamental frequency of the SDOF structure of the structure is 5.0 Hz for the purpose of numerical simulation. It is however worth noting that similar computational simulation results can also be observed for other frequencies. The inherent damping ratio of the SDOF structure is assumed to be 0.02. Based on the research by Wallace *et al.* (2005), the critical values of time delay for stability are approximately calculated as 6.4 msec., so the time delay τ is set to 1 msec. to maintain the stability of the simulation. To verify the effectiveness of the frequency domain based approach with data decimation, no delay compensation method is used. The amplitude error introduced by actuator is set 1.1. The ground motion records, the MU2035 component of the 1994 Northridge earthquake and the CHY101-N component of the 1999 Chichi earthquake, are randomly selected from the PEER Strong Motion Database. The sampling rate for the computational simulation is assumed to be 1024 Hz which is consistent with the state-of-the-art servo-hydraulic equipment. To accommodate different sampling rates from the ground motion records, a first order linear interpreter method is used for resampling the ground motion records from 100 Hz for MU2035 and 200 Hz for CHY101-N to 1024 Hz. The data length after interpolation is 24577 for MU2035 and 92161 for CHY101-N, respectively. Chen *et al.* (2013) showed that the scale of ground motions does not affect the effectiveness of the frequency-domain based approach. The original records from PEER database are therefore used in the numerical simulation of this study. The time history of displacement responses for linear elastic structure subjected to two ground motions are presented in Fig. 1. Also presented in Fig. 1 are the actual structural responses without time delay and amplitude error. It can be observed that the actuator tracking error leads to large discrepancy in simulated structural response. However, this comparison is often not possible since the actual structural response is often not available before or even after the experiments.

Due to different data length, frequency interval in frequency analysis is 0.0313 Hz for MU2035 and 0.0078 Hz for CHY101-N. The values of decimation factor P are selected as 1, 2, 4, 8, 16, 32, 64, 128, 256 and 512, resulting the maximum frequency 512 Hz, 256 Hz, 128 Hz, 64 Hz, 32 Hz, 16 Hz, 8 Hz, 4 Hz, 2 Hz and 1 Hz for the frequency-domain based approach. The amplitude A and the time delay d in frequency-domain evaluation approach with different factors P for the selected

linear structure are presented in Fig. 2.

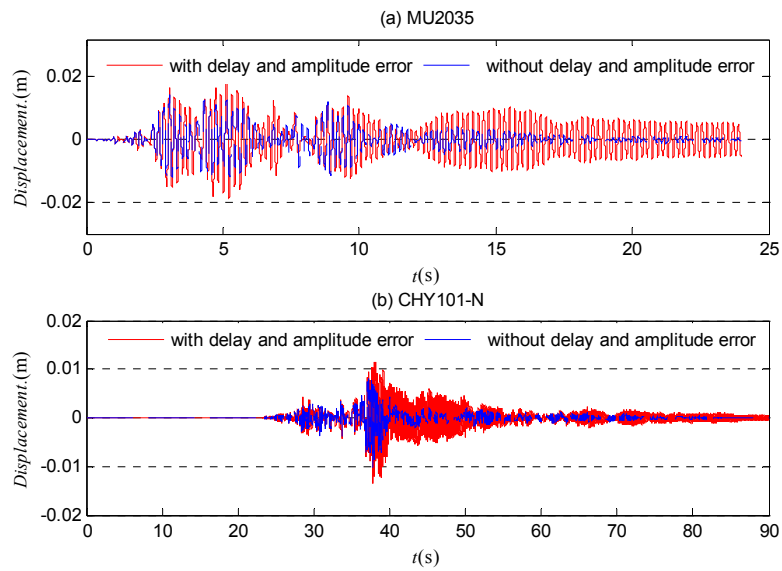


Fig. 1 Time histories of displacement responses for linear elastic structure

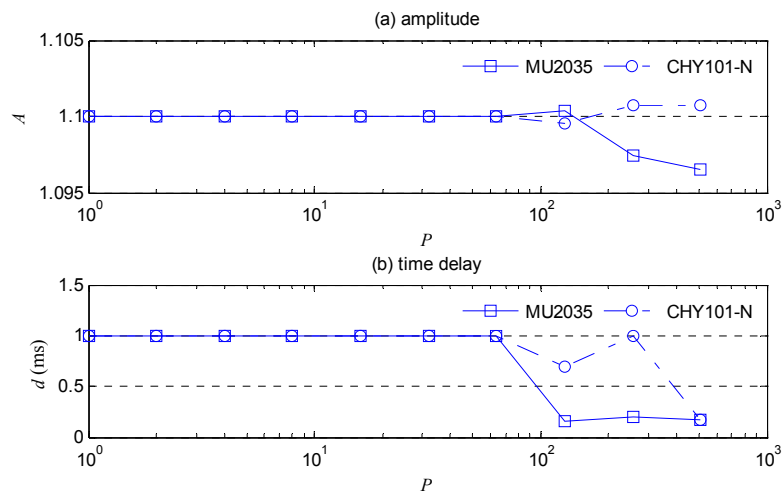


Fig. 2 Frequency analyses with different P for linear structure

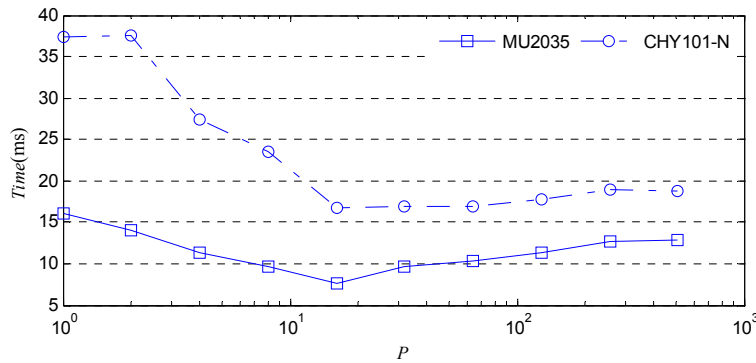


Fig. 3 Computation time with different P for linear structure

When the factor P is equal to 1, the amplitude A is identified to be equal to 1.1 in Fig. 2(a) and the value of equivalent delay d is 1 msec. in Fig. 2(b) for both two simulations, which agrees exactly with the amplitude error and time delay introduced in the computational simulation. It is also observed that the two indices (A and d) are almost the same for all different values of P smaller than 64. This implies that smaller value of the decimation factor P than 64 has little influence on the effectiveness of the frequency response analysis approach. However, when the decimation factor P becomes larger than 128, the theoretical value and simulation results become quite different, indicating that the larger value of P leads to poor accuracy for the approach.

The computation time for the frequency-domain based approach with different factor P is presented in Fig. 3 for the linear elastic structure. For the MU2035 ground motion, the computational efficiency increases with larger P when P is no more than 16. The computation time becomes almost constant when P exceeds 16. This might be attributed to the fact that the reduced computational efforts cannot make up the time required for the data decimation. Similar observation can also be made for the simulation with ground motion CHY101-N. When the value of P is 16, the computation time for the frequency based analysis approach is about 50% of that when the value P is 1, implying that the computational efficiency of the approach is almost doubled by the data decimation technique. The analysis above also indicates that a value of 16 for P is more appropriate for improving computational efficiency while maintaining accurate analysis results.

3.1.2 Nonlinear structure

The influence of decimation factor P is further evaluated for structures with nonlinear behavior. Nonlinear structural behavior usually will lead to larger displacement response than the corresponding linear elastic structure, thereby resulting in larger values for the time-domain based variables such as TI . The nonlinear structural behavior in this study is emulated using the Bouc-Wen model (Wen 1980) as

$$r(t) = \eta \cdot k \cdot x(t) + (1 - \eta) \cdot k \cdot x_y \cdot z(t) \quad (13a)$$

In Eq. (13(a)) x_y is the yield displacement of the experimental substructure and is set to 10 mm; k is the linear elastic stiffness of the experimental substructure and is set to 11.765 kN/mm; η is the

ratio of the post- to pre-yield stiffness of the experimental substructure and is set to 0.01; $x(t)$ is the displacement imposed on the experimental substructure by the integration algorithm; and $z(t)$ is the evolutionary parameter of the Bouc-Wen model governed by the following differential equation

$$x_y \cdot \dot{z}(t) + \gamma |\dot{x}(t)| \cdot z(t) \cdot |z(t)|^{q-1} + \beta \cdot \dot{x}(t) \cdot |z(t)|^q - \dot{x}(t) = 0 \quad (13b)$$

The dimensionless parameters β , γ and q in Eq. (13(b)) control the shape of the hysteretic loop of the experimental substructure and their values are set to 0.55, 0.45 and 2, respectively. Nonlinear SDOF structures with 1.0 Hz natural frequency is considered in the computational analysis for this section. The same MU2035 component from the 1994 Northridge earthquake and the CHY101-N component of the 1999 Chichi are used. It has been shown by Chen *et al.* (2013b) that for the selected Bouc-Wen model, the nonlinear structural behavior may help stabilize the real-time hybrid simulation with delay. The time delay τ is set to be 5 msec. for the computational simulation. The time history of displacement responses for the nonlinear structure subjected to two ground motions are presented in Fig. 4. Smaller differences can be observed than those in Fig. 1 for the corresponding linear elastic structure. This is consistent with findings from previous research that nonlinear structural behavior during real-time hybrid simulation can help reduce the response error due to the actuator delay (Chen *et al.* 2013b).

Fig. 5 presents the influence of decimation factor P on frequency response analysis for the nonlinear structure. Similar results to those for the corresponding linear structure in Fig. 2 can be observed. When the value of P is equal to 1.0, analysis of the simulation with MU 2035 gives the values of A and d equal to 1.102 and 5.0 msec., respectively. The relative errors are both less than 1% when compared with the theoretical values of 1.1 and 5 msec. This again confirms that the frequency-domain based approach can provide accurate error identification for real-time hybrid simulations involving both linear and nonlinear structural behavior. When the value of P increases but smaller than 128, it can be observed that the amplitude parameter A in Fig. 5(a) and the equivalent delay d in Fig. 5(b) maintains almost constant around 1.1 and 5 msec., respectively. For the value of P larger than 128, analysis results of the simulation with MU2035 shows significant difference (about 10% relative error) from the theoretical values. This is also consistent with the finding from Fig. 2. However, the same frequency analysis approach still provides accurate results close to theoretical values for the simulation with CHY101-N, which is different from that in Fig. 2 and could be attributed to the nonlinear structural behavior. Fig. 5 implies that the effectiveness of the frequency-domain based approach is not affected by the data decimation for the value of P smaller than 128.

The computation time corresponding to different decimation factor P is presented in Fig. 6. The same trend as that in Fig. 3 can be observed, where the computation time decreases with the increase of P when the value of decimation factor P between 2 and 16, while it has little change when P is larger than 16. A value of 16 for P is again shown to improve computational efficiency without decreasing the accuracy of the analysis results.

In the above analysis, the total calculation time mainly consists of two parts, namely the time for data decimation and the time for frequency domain evaluation (FDE). Data decimation reduces the time consumed in the FDE, while on the other hand, it takes some time to perform the decimation. Therefore, if the time saved through data decimation in the FDE can not make up the consumed time for data decimation, the total computational efficiency would not be improved. Fig. 7 shows the computational time for data decimation with different values of P for nonlinear structure. As shown in Fig. 7, when P is 1, the time is almost 0 msec.; as P increases, the time

spent in data decimation in general grows. Due to data decimation, the total computation time would not become zero.

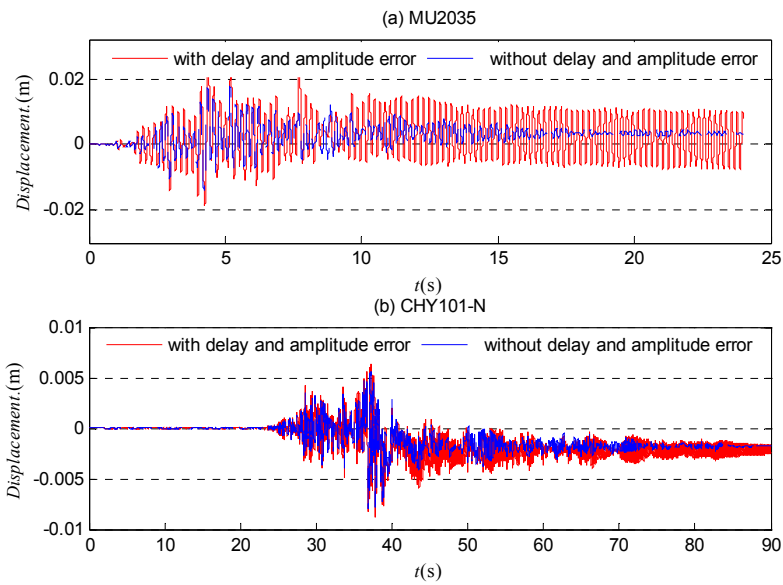


Fig. 4 Time histories of displacement responses for nonlinear structure

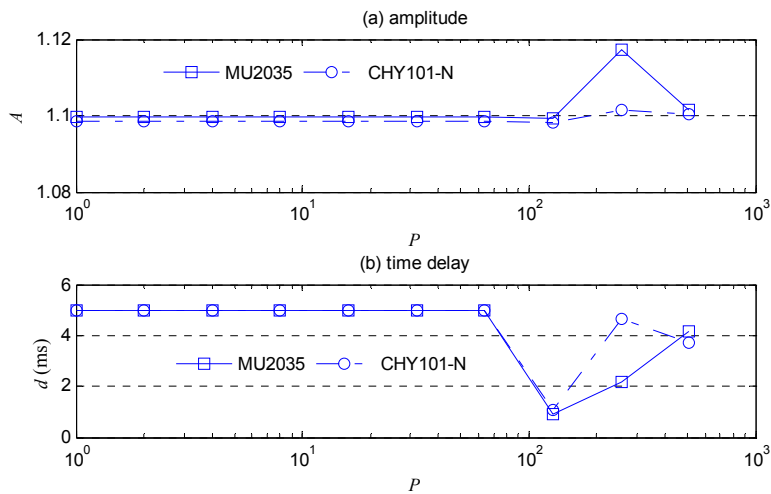


Fig. 5 Frequency-domain analysis with different P for nonlinear structure

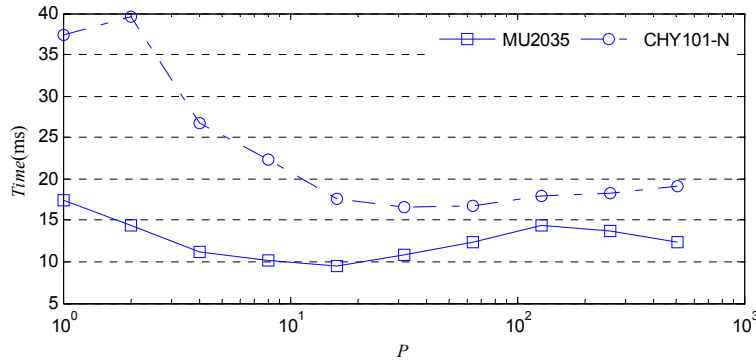


Fig. 6 Computation time with different P for nonlinear structure

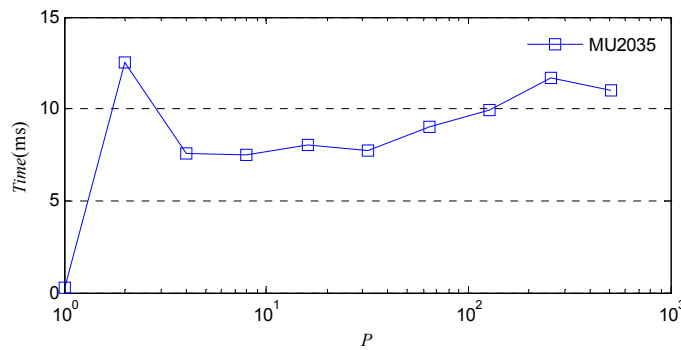


Fig. 7 Relationship between computational time of decimation and P (MU2035) for nonlinear structure

3.2 Application to real-time hybrid simulation results

The experiments for a SDOF moment resisting frame (MRF) with an elastomeric damper conducted at Lehigh University (Chen and Ricles 2010) were used to further verify the effectiveness of data decimation technique (Ricles 2009). The SDOF MRF was used as analytical substructure and the elastomeric damper was tested as experimental substructure. The SDOF MRF has a mass of 503.4 metric tons, an elastic natural frequency of 0.77 Hz, and an inherent viscous damping ratio of 0.02. The elastomeric damper has a load capacity of 200 kN with a stroke of 584 mm. The restoring force of the SDOF MRF is calculated by the Bouc-Wen model described previously in Eqs. (13(a)) and (13(b)). The N169E component of the 1994 Northridge earthquake recorded at Canoga Park was selected as the ground motion, and scaled the maximum magnitude of acceleration to 0.322 m/s^2 to satisfy the limits imposed by the servo-hydraulic equipment (Chen and Ricles 2010). The explicit unconditionally stable CR integration algorithm was used for the real-time hybrid simulations (Chen and Ricles 2008a, b). The inverse compensation method for different actuator delay estimates α_{es} (15, 29 and 45) was used to negate the effect of servo-hydraulic dynamics. The experimental results of the tests are presented in Fig. 8, where the

moment resisting frame is observed to have the maximum displacement of about 36 mm. The residual displacement of 22 mm indicates that nonlinear structural behavior occurred during the simulation.

The data length from experimental results is 51160 resulting in a frequency interval 0.0156 Hz for the frequency-domain based approach. Data decimation factor P is again selected as 1, 2, 4, 8, 16, 32, 64, 128, 256 and 512. The results of two indices (A and d) in frequency-domain evaluation approach are presented in Fig. 9 with different decimation factor P . Slight different values of A are observed in Fig. 9(a) between 1.00 and 1.02, implying that the actuator tracking has almost zero amplitude error for all three real-time hybrid simulations. The time delay d in Fig. 9(b) shows almost constant values of -15.6 msec., -0.4 msec. and 13.2 msec. for the three tests with α_{es} equal to 15, 29 and 45, respectively. Unlike the computational simulation results, larger values of the decimation factor P than 256 are observed to lead to very small differences in the analysis results when compared with those of P equal to 1.0.

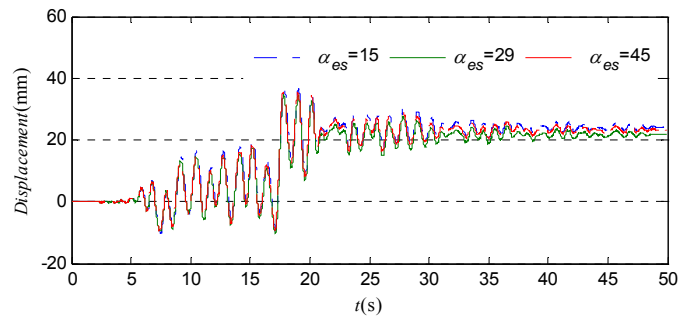


Fig. 8 Displacement responses from experimental results

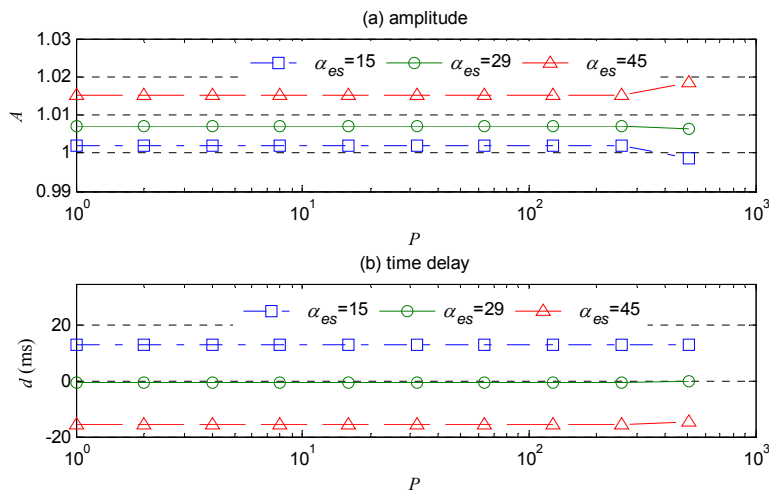


Fig. 9 Frequency analyses with different P for real-time hybrid simulation results

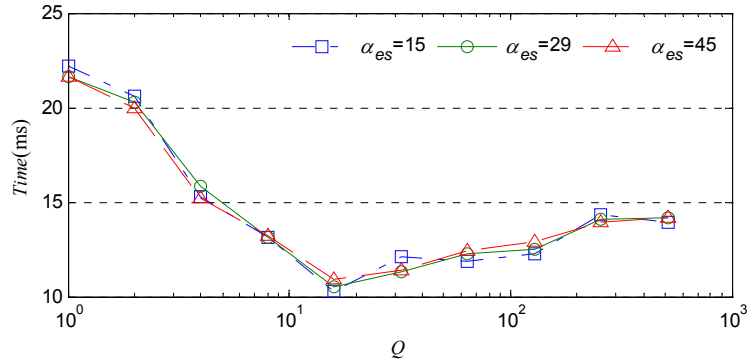


Fig. 10 Computation time with different P for real-time hybrid simulation results

The computation time in calculation with different decimation factor P for experiments is presented in Fig. 10. The computation time for the frequency analysis approach is observed to decrease for the value of P between 2 and 16 and then remain constant when P is larger than 16. It can then be reasonably argued that a value of 16 for P should be used to improve computational efficiency without decreasing the accuracy of the analysis results.

4. Frequency decimation factor Q

After the data are translated from time-domain to frequency-domain using *FFT*, equivalent frequency f^{eq} in Eq. (7) and *FEI* in Eq. (12) are weighted at each frequency intervals. For a real-time hybrid simulation with 20 seconds ground motion, the number of frequencies to be weighted in Eqs. (7) and (12) could be as high as 10240. In this section a frequency decimation factor Q is introduced to increase the frequency interval so as to reduce the number of frequencies to be weighted. In other words, only selected frequencies instead of all the frequencies are weighted in the frequency-domain based approach to calculate the amplitude error and time delay. Taking Q equals 2 for example, one frequency out of every two frequencies is used for the FDE. Through the frequency decimation factor, computation time consumed for the FDE is expected to decrease.

4.1 Computational simulation

The data from computational simulations presented in Figs. 1 and 3 are used to numerically evaluate the efficiency of the frequency decimation for the frequency domain based approach. For the purpose of analysis, the P factor is set to be equal to 1, which means the data are not decimated in time-domain and the max frequency is 512 Hz for the analysis presented in the section.

4.1.1 Linear elastic structure

The values of decimation factor Q are selected to be 1, 2, 4, 8, 16, 32, 64, 128, 256 and 512, resulting in the frequency interval of 0.0313 Hz, 0.0626 Hz, 0.1252 Hz, 0.2504 Hz, 0.5008 Hz, 1.0016 Hz, 2.0032 Hz, 4.0064 Hz, 8.0128 Hz, 16.0512 Hz for MU2035; and 0.0078 Hz, 0.0156 Hz,

0.0313 Hz, 0.0626 Hz, 0.1252 Hz, 0.2504 Hz, 0.5008 Hz, 1.0016 Hz, 2.0032 Hz, 4.0064 Hz for CHY101-N. The results of the indices in frequency-domain evaluation approach, A and d , are presented in Fig. 11 for different values of Q .

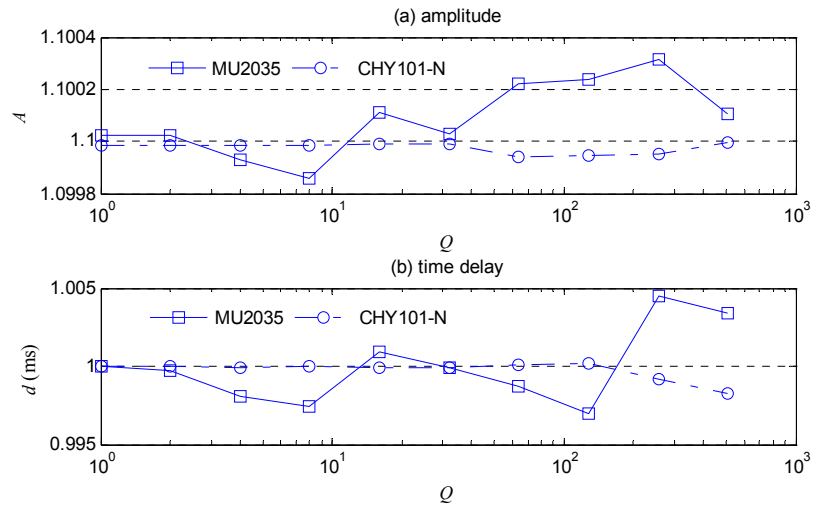


Fig. 11 Frequency analyses with different Q for linear structure

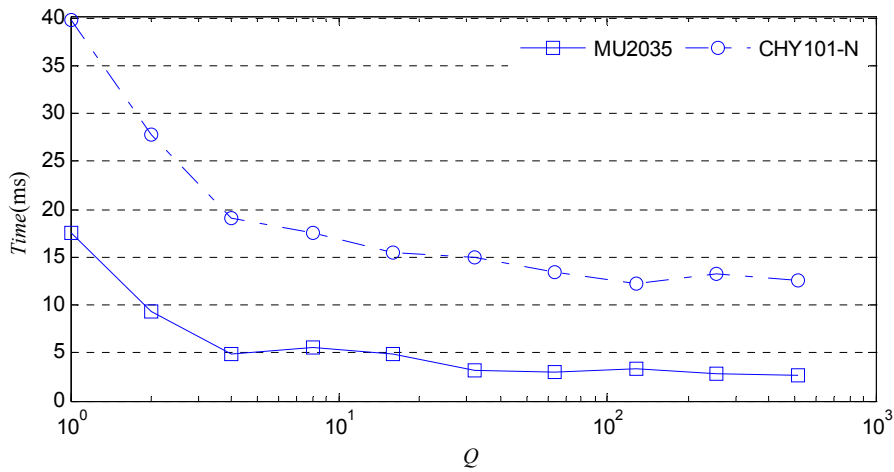


Fig. 12 Computation time with different decimation factor Q for linear structure

When the value of Q is 1 (i.e., no decimation is used), the theoretical value of A and d , are 1.1 and 1 msec., respectively, which are identical with the analysis results in Fig. 11(a) for A and Fig. 11(b) for d . For the value of Q between 2 and 512, Fig. 11 shows almost same value of A and slight different values of d (0.5% relative error). The frequency decimation technique leads to almost same analysis results for the simulations with different ground motions when the frequency decimation technique is used with Q between 1 and 128. For the value of Q larger than 256, the frequency response analysis results start deviating from the theoretical values and show different values for the two ground motions. The computation time in Fig. 12 is observed to decrease monotonically with the increase of Q when Q is smaller than 16, and remain constant for larger values of Q . When the value of Q is equal to 16, Fig. 12 shows that the computation time is reduced to about 25% of that when the factor Q is equal to 1.0, implying that the computational efficiency is significantly improved.

4.1.2 Nonlinear structure

The frequency decimation technique is again evaluated for the nonlinear structure and the analysis results are presented in Fig. 13. Similar results to those in Fig. 11 can be observed. The amplitude and equivalent delay agree well with the theoretical values with maximum relative errors smaller than 0.1% for both A and d when the decimation factor Q is smaller than 32. Combined with findings from Fig. 11, it is demonstrated that the effectiveness of the frequency-domain based approach is not affected by the frequency decimation. The difference in Fig. 13 however can be observed to increase substantially when the decimation factor Q is larger than 32, where the relative error is 0.1% for A and 1% for d . It is therefore recommended to use no larger value of Q than 32. The computation time for different decimation factor Q is presented in Fig. 14, where the computation time for nonlinear structure with different decimation factor Q has the same trend as that for the corresponding linear structure. A value of 16 for Q is demonstrated to enable improved computational efficiency without decreasing the accuracy of the analysis results.

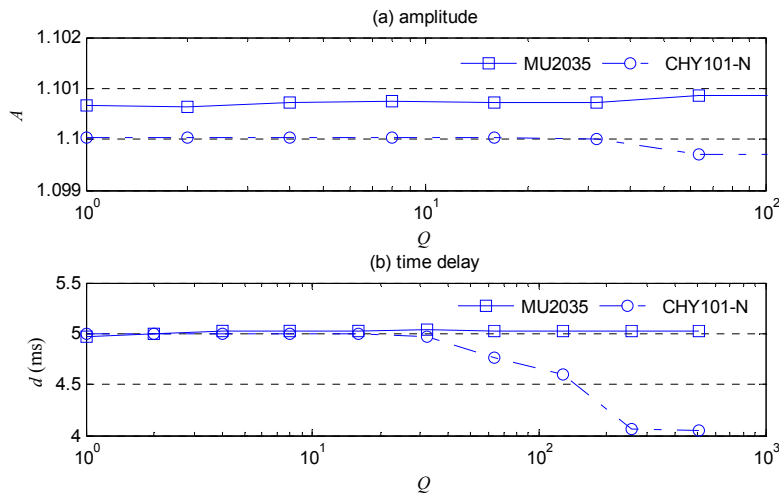


Fig. 13 Frequency analyses with different factor Q for nonlinear structure

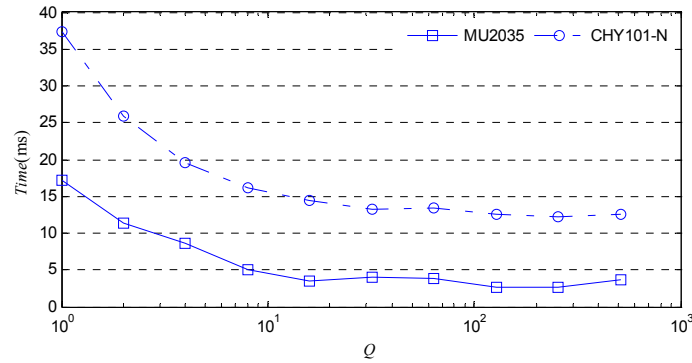


Fig. 14 Computation time with different decimation factor Q for nonlinear structure

4.2 Application to real-time hybrid simulation results

The real-time hybrid simulation results in Fig. 8 are used to verify the effectiveness of frequency decimation. Frequency decimation factor Q is again set to 1, 2, 4, 8, 16, 32, 64, 128, 256, 512, resulting frequency interval 0.0156Hz, 0.0313Hz, 0.0626Hz, 0.1252Hz, 0.2504Hz, 0.5008Hz, 1.0016Hz, 2.0032 Hz, 4.0064 Hz and 8.0128 Hz. The results of A and d from the frequency-domain evaluation approach are presented from Fig. 15 for different values of Q . When frequency decimation factor Q is set to 1, the analysis results in Fig. 15 are also exactly same as those in Fig. 9. In Fig. 15, the values of A and d from the frequency-domain approach have almost same values when the factor Q is smaller than 16. For a larger value of Q than 32, the analysis results start to deviate from those for Q equal to 1 and are considered to be more inaccurate. The computation time is also presented in Fig. 16 for different values of Q . Similar to that in Fig. 14, the computation time decreases monotonically with the increase of decimation factor Q when the factor Q is smaller than 32, and then remains almost constant for larger values of Q . The value of 32 for Q is demonstrated to greatly improve computational efficiency by almost four times without decreasing the accuracy of the analysis results, which is consistent with the findings from the numerical simulation.

5. Combination of the two decimation factors

5.1 Computational simulation

The analysis above shows that both data and frequency decimation can separately improve the computational efficiency for the frequency-domain based approach to evaluate the effect of actuator delay in real-time hybrid simulation. In this section, analysis is conducted to explore if combining the two decimation techniques could lead to more significant improvement on the computational efficiency. The maximum values of P and Q are selected to be 64 and 32, respectively, based on the analysis from previous sections. The results of A and d are presented in

Figs. 17 and 18 with different decimation factors for the linear structure. Same analysis results as those in Figs. 2 and 11 can be observed in Figs. 17 and 18, where the analysis results agree well with the theoretical values with relative errors less than 1%. Combining the data and frequency decimation is shown to not affect the effectiveness of the frequency-domain based approach. Comparing the separate effect of the two factors P and Q on the frequency-domain based approach, it can also be observed in Figs. 17 and 18 that the frequency decimation factor Q has more impact on the accuracy of frequency response analyses than the data decimation factor P . The analysis results of A and d vary for different factor Q but remain almost constant for factor P .

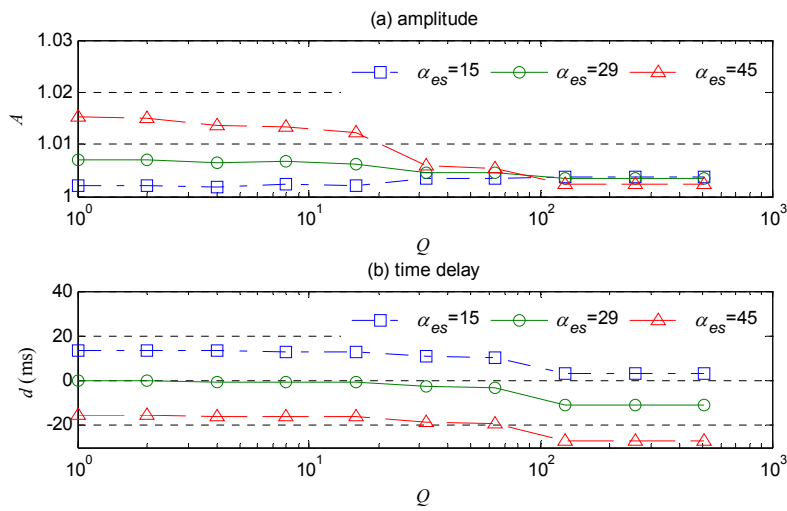


Fig. 15 Frequency analyses results with different Q

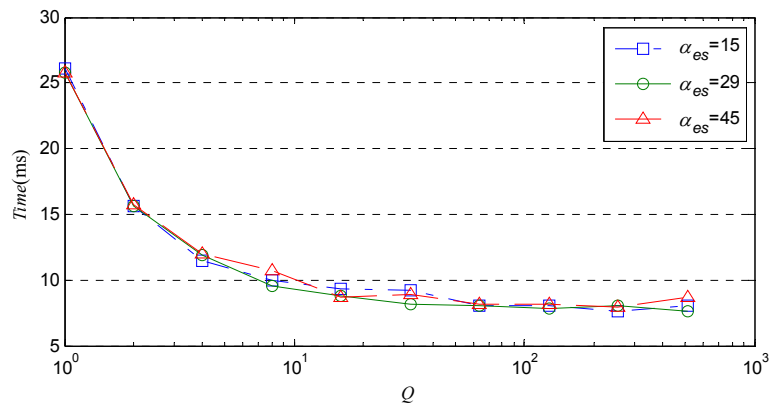


Fig. 16 Computation time with different decimation factor Q for experiments

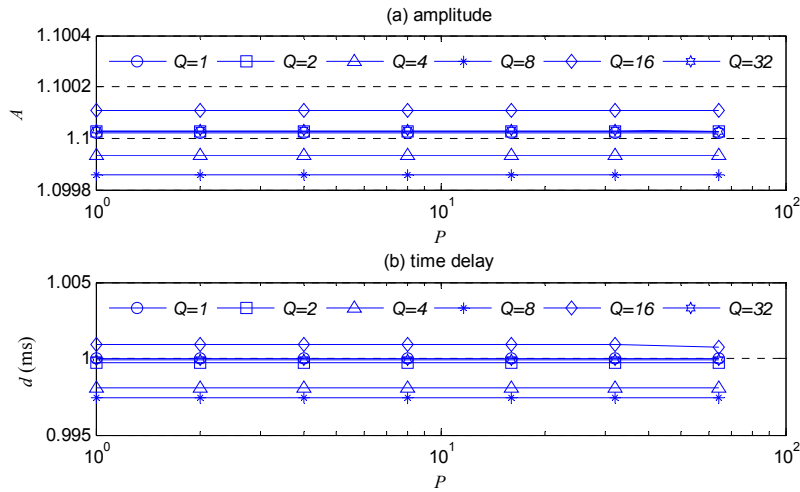


Fig. 17 Frequency analyses for linear structure (MU2035)

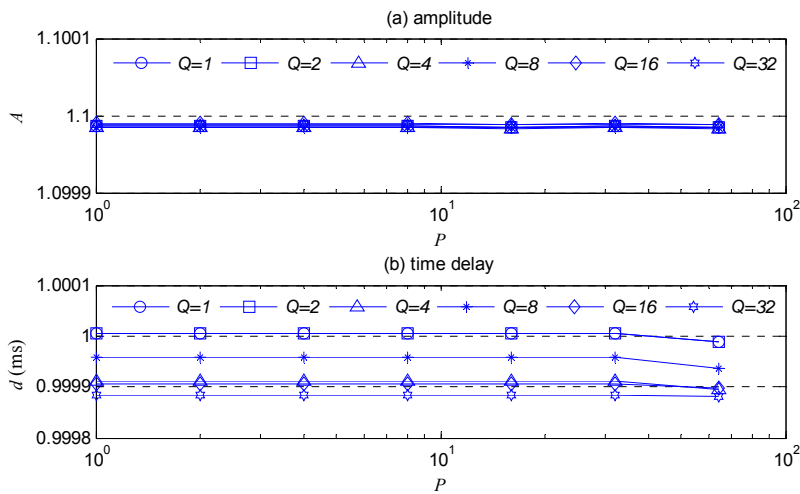


Fig. 18 Frequency analyses for linear structure (CHY101-N)

The computation time with regards to different P and Q is presented in Table 1, where it is observed that increasing the values of Q results in faster decrease in computation time than increasing the values of P . Figs. 19 and 20 show the frequency-domain analysis results with different decimation factors for nonlinear structure. Similar results to those in Figs. 4 and 13 can be observed implying that nonlinear structural behavior does not affect the effectiveness of the frequency domain based approach when both data and frequency decimation are used. The computation time for combining different P and Q for nonlinear structure is presented in Table 2.

Similar trend can be observed as those for linear structure, implying again that the nonlinear structural behavior does not affect the performance of the frequency domain based approach. To achieve accurate analysis results with minimal computation time, Figs. 19 and 20 indicate that the decimation factors P and Q should be no larger than 64 and 16, respectively. Similar to that observed in Table 1, when the values of P and Q are equal to 1 and 16, respectively, the computation time for the frequency response analysis is reduced to about 30% of that for both P and Q equal to 1. To balance the accuracy and efficiency, the value of the Q is recommended to select 16. If the computation time for analysis is still too large for simulation, the value of P equal to 16 can be used to further improve the efficiency of the analysis.

Table 1 Computation time with different P and Q for linear structure (msec.)

$Q \backslash P$	MU2035						CHY101-N					
	1	2	4	8	16	32	39.4	26.3	19.7	16.4	14.8	14.3
1	16.9	8.4	6.4	5.5	5.0	4.6	40.9	34.3	31.5	29.6	28.7	28.3
2	13.5	11.8	10.7	10.2	10.0	9.9	29.2	26.0	24.4	23.6	23.2	22.9
4	9.7	8.8	8.4	8.1	8.0	7.9	25.0	23.6	22.6	22.2	21.9	21.8
8	8.8	8.4	8.2	8.1	8.1	8.0	20.4	19.6	19.2	19.1	18.9	18.9
16	10.1	9.9	9.8	9.8	9.8	9.7	20.6	20.2	20.1	19.9	19.9	19.8
32	10.7	10.6	10.6	10.5	10.5	10.5	21.9	21.7	21.6	21.6	21.5	21.5
64	12.6	12.6	12.5	12.5	12.5	12.5	39.4	26.3	19.7	16.4	14.8	14.3

Table 2 Computation time with different P and Q for nonlinear structure (msec.)

$Q \backslash P$	MU2035						CHY101-N					
	1	2	4	8	16	32	1	2	4	8	16	32
1	13.8	7.0	5.1	4.6	4.1	3.8	42.9	27.7	20.1	16.5	14.6	13.7
2	12.0	10.3	9.5	9.1	8.8	8.7	41.4	35.0	31.4	29.7	28.9	28.4
4	9.3	8.5	8.0	7.8	7.7	7.7	28.4	25.5	23.5	22.6	22.1	22.0
8	8.8	8.4	8.2	8.1	8.1	8.0	26.9	25.5	24.5	24.1	23.8	23.7
16	9.2	9.0	8.9	8.9	8.8	8.8	19.8	18.8	18.7	18.4	18.2	18.2
32	11.0	10.8	10.8	10.7	10.7	10.7	20.9	20.5	20.3	20.2	20.2	20.1
64	11.6	11.6	11.5	11.5	11.5	11.5	19.6	19.5	19.3	19.3	19.2	19.2

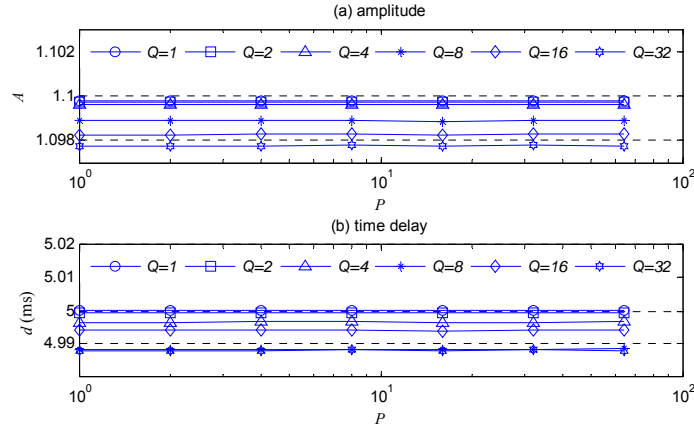


Fig. 19 Frequency analyses for nonlinear structure (MU2035)

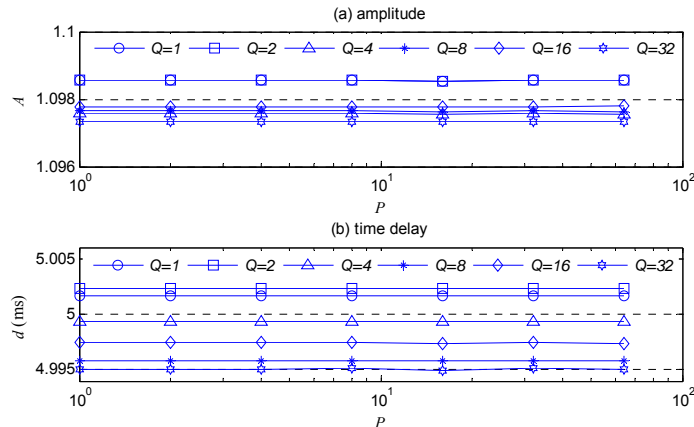


Fig. 20 Frequency analyses for nonlinear structure (CHY101-N)

5.2 Application to real-time hybrid simulation results

The effect of combining the two factors to improve the computational efficiency is evaluated using the same experimental tests described previously. The analysis results are presented in Fig. 21 to Fig. 23, for tests with $\alpha_{es}=15, 29$, and 45 , respectively. Similar results can be observed in Fig. 21 to Fig. 23 that combining the decimation factors P and Q does not affect the accuracy of analysis results when the values of P and Q are no larger than 64 and 16 , respectively. This is consistent with findings from previous numerical simulation. Moreover, the computation time presented in Tab. 3 indicates that combining the two factors can help reduce the computation time as large as 40% . When the values of P and Q are equal to 1 and 16 , respectively, the computation time for the frequency response analysis is reduced to about 35% of that for both P and Q equal to 1 .

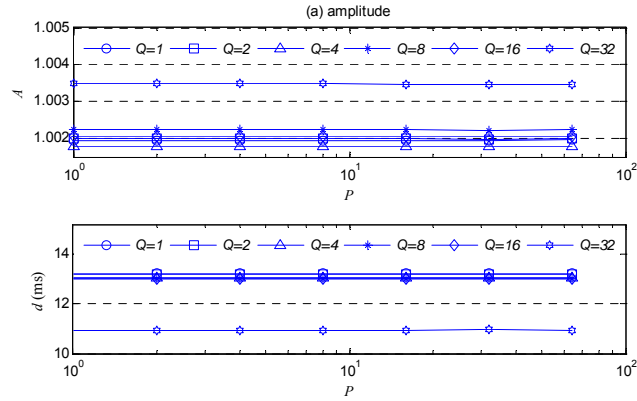


Fig. 21 Frequency analysis results with combination of the two factors ($\alpha_{es}=15$)

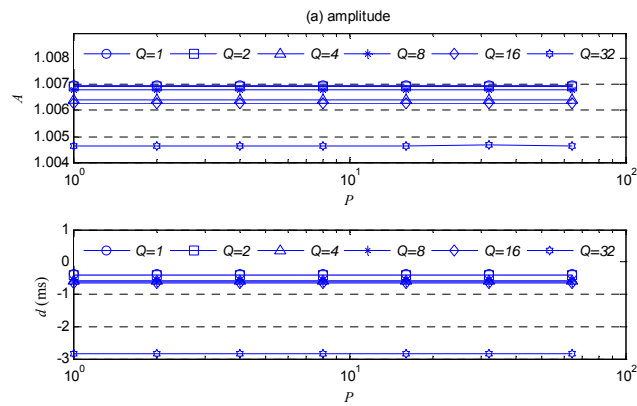


Fig. 22 Frequency analysis results with combination of the two factors ($\alpha_{es}=29$)

Table 3 Computation time with different P and Q for experiments (msec.)

Q	$\alpha_{es}=15$					$\alpha_{es}=29$					$\alpha_{es}=45$				
	2	4	8	16	32	2	4	8	16	32	2	4	8	16	32
1	16.1	12.5	10.6	9.5	9.0	15.4	11.3	9.4	8.5	8.0	16.3	12.4	10.6	9.6	9.1
2	20.5	18.7	17.7	17.1	16.9	20.6	18.8	17.7	17.1	16.9	20.5	18.6	17.7	17.2	16.9
4	17.4	16.5	15.9	15.7	15.5	17.6	16.6	16.0	15.8	15.6	17.3	16.4	15.8	15.6	15.5
8	15.8	15.3	15.1	14.9	14.9	15.5	15.0	14.8	14.6	14.6	15.6	15.1	14.9	14.7	14.7
16	14.6	14.4	14.2	14.2	14.1	13.7	13.5	13.3	13.3	13.2	14.1	13.9	13.7	13.7	13.6
32	14	13.8	13.8	13.7	13.7	13.9	13.8	13.7	13.6	13.6	14.6	14.4	14.4	14.3	14.3
64	15.4	15.3	15.2	15.2	15.2	14.1	14.1	14.1	14.0	14.0	14.6	14.6	14.5	14.5	14.5

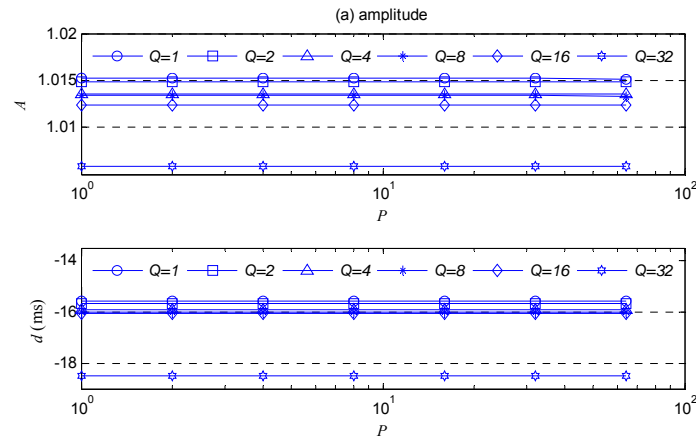


Fig. 23 Frequency analysis results with combination of the two factors ($\alpha_{es}=45$)

6. Conclusions

Compared with existing time-domain based techniques, the frequency-domain evaluation approach provides a more quantitative assessment of actuator tracking in terms of amplitude error and time delay. In this paper, two decimation techniques, data decimation and frequency decimation, are analyzed to improve the computational efficiency of the frequency-domain evaluation approach. Numerical simulations are first conducted and experimental tests are then used to verify the effectiveness of the two decimation techniques. It is demonstrated that both decimation techniques can help reduce the computation time thus improving the computational efficiency. Nonlinear structural behavior does not affect the frequency-domain based approach with decimation technique.

Compared with data decimation factor P , frequency decimation factor Q has more influence on the accuracy and efficiency of the analysis. To balance the accuracy and efficiency, it is recommended to take the value of P as 16. If the computation time for analysis is still too large for simulation, the value of Q can be larger than 16 to further improve the efficiency of the analysis. Analyses for computational simulation and experimental results show that the two decimation techniques can help reduce the computational time as much as 60%.

The future work of this ongoing work include: (1) integrating the proposed approach with more advanced signal processing techniques to further reduce the required computation time; (2) applying the proposed method in structures with more complicated nonlinear properties (i.e., with stiffness degradation) and in structures with multiple degrees of freedom; (3) further reduction in the computation time by selecting some key frequencies. As a result, the analysis results in the present study can be integrated into the frequency-domain based approach and applied towards real-time on-line actuator tracking assessment.

Acknowledgements

The support from the Natural Science Foundation of China under Grant No. 51378107, the Priority Academic Program Development of Jiangsu Higher Education Institutions and the Excellent Doctoral Dissertation Foundation of Southeast University are gratefully acknowledged.

The third author would also like to acknowledge the support from the National Science Foundation under the award number CMMI-1227962. The real-time hybrid simulation results presented in this study were conducted during the corresponding author's post-doctoral study at the NEES Real-Time Multi-Directional (RTMD) Facility at Lehigh University. The authors would like to express their appreciation to Lehigh RTMD testing facility for the permission of the use of the experimental data.

References

- Ahmadizadeh, M., Mosqueda, G. and Reihorn, A.M. (2008), "Compensation of actuator delay and dynamics for real-time hybrid structural simulation", *Earthq. Eng. Struct. D.*, **37**(1), 21-42.
- Bonnet, P.A, Lim, C.N., Williams, M.S., Blakeborough, A., Neild, S.A., Stoten, D.P. and Taylor, C.A. (2007), "Real-time hybrid experiments with newmark integration, MCSmd outer-loop control and multi-tasking strategies", *Earthq. Eng. Struct. D.*, **36**(1), 119-141.
- Bracewell, R.N. (2000), *The Fourier Transform and Its Applications*, 3rd Ed., Boston, McGraw-Hill.
- Carrion, J.E., Spencer, B.F. (2006), "Real-time hybrid testing using model-based delay compensation", *Proceeding of the 4th International Conference on Earthquake Engineering*, October Taipei Taiwan.
- Chen, C. and Ricles, J.M. (2007), "Stability analysis of SDOF real-time hybrid testing systems with explicit integration algorithms and actuator delay", *Earthq. Eng. Struct. D.*, **37**(4), 597-613.
- Chen, C. and Ricles, J.M. (2008a), "Development of direct integration algorithms for structural dynamics using discrete control theory", *J. Eng. Mech. - ASCE*, **134**(8), 676-683.
- Chen, C. and Ricles, J.M. (2008b), "Stability analysis of SDOF real-time hybrid testing systems with explicit integration algorithms and actuator delay", *Earthq. Eng. Struct. D.*, **37**(4), 597-613.
- Chen, C. and Ricles, J.M. (2010), "Tracking error-based servo-hydraulic actuator adaptive compensation for real-time hybrid simulation", *J. Eng. Mech. - ASCE*, **136**(4), 432-440.
- Chen, C., Ricles, J.M., Sause, R. and Christenson, R. (2010), "Experimental evaluation of an adaptive actuator control technique for real-time simulation of a large-scale magneto-rheological fluid damper", *Smart Mater. Struct.*, **19**, 025017.
- Chen, C., Ricles, J.M. and Guo, T. (2012), "Improved adaptive inverse compensation technique for real-time hybrid simulation", *J. Eng. Mech. - ASCE*, **138**(12), 1432-1446.
- Chen, C. and Sharma, R. (2012), "A reliability assessment approach for real-time hybrid simulation results", *Canadian Society for Civil Engineering annual conference and 3rd International Structural Specialty Conference*, June 6-9, Edmonton, Alberta, Canada.
- Chen, C., Guo, T. and Xu, W. (2013a), "Frequency response evaluation of cumulative effects of servo-hydraulic dynamics in real-time hybrid simulation", *Eng. Struct.*, submitted, under review.
- Chen, C., Valdovinos J. and Santillano, H. (2013b), "Reliability assessment of real-time hybrid simulation results for seismic hazard mitigation", *Proceeding of the Structures Congress*, May 2-4, Pittsburgh, PA.
- Chen, C., Guo, T. and Xu, W.J. (2014), "Developing a frequency-domain based approach for actuator tracking assessment in real-time hybrid simulation", Network for Earthquake Engineering Simulation (NEES) (distributor). Dataset. DOI: 10.4231/D37M0409H.
- Darby, A.P., Blakeborough, A. and Williams, M.S. (1999), "Real-time substructure tests using hydraulic actuators", *J. Eng. Mech. - ASCE*, **125**(10), 1133-1139.
- Darby, A.P., Blakeborough, A. and Williams, M.S. (2002), "Stability and delay compensating for real-time

- substructure testing”, *J. Eng. Mech. - ASCE*, **128**(12), 1276-1284.
- Guo, T., Chen, C., Xu, W. and Sanchez, F. (2014), “A frequency response analysis approach for quantitative assessment of actuator tracking for real-time hybrid simulation”, *Smart Mater. Struct.*, **23**(4), 045042.
- Harris, F.J. (1978), “On the use of windows for harmonic analysis with the discrete Fourier transform”, *Proc. IEEE*, **66**, 51-83.
- Hessabi, R.M. and Mercan, O. (2012), “Phase and amplitude error indices for error quantification in pseudodynamic testing”, *Earthq. Eng. Struct. D.*, **41**(10), 1347-1364.
- Horiuchi, T., Inoue, M., Konno, T. and Namita, Y. (1999), “Real-time hybrid experimental system with actuator delay compensation and its application to a piping system with energy absorber”, *Earthq. Eng. Struct. D.*, **28**(10), 1121-1141.
- MATLAB. (2009), *The Math Works, Inc.*, Natick, MA.
- Mercan, O. (2007), *Analytical and experimental studies on large scale real-time pseudodynamic testing*, Ph.D. dissertation, Dept. of Civil and Environmental Engineering, Lehigh Univ., Bethlehem, Pa.
- Mosqueda, G., Stojadinovic, B. and Mahin, S.A. (2007a), “Real-time error monitoring for hybrid simulation. Part I: methodology and experimental verification”, *Earthq. Eng. Struct. D.*, **133**(8), 1100-1108.
- Mosqueda, G., Stojadinovic, B. and Mahin, S.A. (2007b), “Real-time error monitoring for hybrid simulation: Part II: structural response modification due to errors”, *Earthq. Eng. Struct. D.*, **133**(8), 1109-1117
- Nakashima, M., Kato, H. and Takaoka, E. (1992), “Development of real-time pseudodynamic testing”, *Earthq. Eng. Struct. D.*, **21**(1), 79-92.
- PEER Strong Ground Motion Database (2013), <http://peer.berkeley.edu>
- Phillips, B.M. and Spencer, B.F. (2012), “Model-based multi-actuator control for real-time hybrid simulation”, *J. Eng. Mech. - ASCE*, **139**(2), 219-228.
- Ricles, J.M. (2009), “Advanced servo-hydraulic control and real-time testing of damped structures”, Network for Earthquake Engineering Simulation (NEES) (distributor). <http://nees.org/warehouse/project/711>.
- Wallace, M.I., Sieber, J., Neild, S.A., Wagg, D.J. and Krauskopf, B. (2005), “Stability analysis of real-time dynamic substructuring using delay differential equation models”, *Earthq. Eng. Struct. D.*, **34**(15), 1817-1832.
- Wen, Y.K. (1980), “Equivalent linearization for hysteretic systems under random excitation”, *T ASAE*, **47**, 150-154.